Microsyst Technol (2012) 18:437–442
DOI 10.1007/s00542-012-1446-8

TECHNICAL PAPER

Enhancement of PZT embedded swing arm actuator using integrated read/write performance and actuation

Yu-Cheng Lin · Po-Chien Chou · Stone Cheng

Received: 7 November 2011 / Accepted: 25 January 2012 / Published online: 14 February 2012

Abstract The current technological challenges associated with the rotary-type seesaw arm actuator for small-form-factor (SFF) disk drives are the small skew focusing, which causes off-axis aberrations and reduces optical quality. This article develops a novel design for a seesaw arm actuator and suspension assembly that is based on a micro-PZT actuator to position pickup head. Dual-stage actuation relaxes the dynamic requirement on the focusing stroke. The proposed actuator with a tilt-compensation mechanism uses a PZT bender to drive pickup head focusing. This combined system, optical module and dual stage actuator, is effectively self-aligned the optical axis for read/write performance in both experiment and simulation result. Finite element modeling and dynamic measurements reveal significant improvements in the actuator bandwidth with and without micro-PZT actuator compensation.

1 Introduction

Various optical and mechanical design factors are considered to meet SFF requirements, as well as optical aberrations inhibit enhancement of the optical sensitivity (Kim et al. 2009a, b).

Many researches develop a swing arm actuator to solve the aberration problem (Lee et al. 2005; Blankenbeckler et al. 2004; Chou et al. 2010a, b). This swing arm actuator consists of a suspension, voice coil motor (VCM) of focusing and tracking, and bearing to provide two-biaxial rotations (Fig. 2), It is possible to maintain a uniform gap in tracking operation by a tracking coil with ring yoke to act on a fan-shape magnet array. It not only provides high magnetic flux but also increase precision of the tracking position (Lin et al. 2011). However, swing arm actuator is especially limited by small skewed actuation in focusing. Hence, this paper analyzes the performance of a dual-stage seesaw arm actuator which is embedded a PZT suspension and designed to extend the effective dynamic range of read/write performance (Ko et al. 2006; Cho et al. 2002). This design includes a novel optical compensation structure, which enables the focus position to be driven by PZT actuation. Skew angle compensation simplifies mechanism to enhance the sensing performance and off-optical axis capacity over those provided by other actuator designs. Finite element modeling for modal analysis is conducted to investigate the dynamic characteristics of the seesaw arm actuator with and without an embedded micro-PZT actuator. Experimental measurements in the actuator focusing direction are made to compare dynamically two prototype actuators. The concepts are proven by numerical simulations and experimental validation.

2 Sensor validation and tilt detection

The basis of the actuator validation scheme is using the optical module to elucidate the tilt-compensation mechanism (Shih et al. 2005; Hou et al. 2011). Figure 1a schematically depicts the integ rated optics. After the 45° turning mirror (not shown) reflects the horizontal laser beam upwards, micro prisms 2 and 1 redirect the beam

Y.-C. Lin · P.-C. Chou · S. Cheng (✉)
Department of Mechanical Engineering, National Chiao Tung University, Hsinchu 30010, Taiwan, R.O.C.
e-mail: stonecheng@mail.nctu.edu.tw

Y.-C. Lin
e-mail: owan0518@hotmail.com

P.-C. Chou
e-mail: arthurking8@msn.com

toward a holographic optical element (HOE). In the optical return path, the returning beam is diffracted by the HOE patterns and reflected by micro prism 1 to micro prism 2. Finally, the returning beam is projected onto the quadrant photo-detector and generates the focusing error signal (FES) to measure the tilt angle.

The results of the simulation are plotted as FES (S-curve), obtained from the light intensity variations of the quadrant photo-detector. Figure 1b shows the skew movement of the seesaw arm versus the angle of the reference beam. When the tilt angle exceeds the maximal optical tolerance, the diffraction efficiency of each HOE is close to zero. The black line is the theoretical S-curve (0°) and the blue line (±0.3°) is obtained using the skew focusing mechanism. During readout, the tilt of seesaw arm causes coma aberration due to the incident beam being tilted which degrades the jitter signal (Knittel et al. 2009). Hence, an effective tilt compensation scheme is developed to enable sensing. The red line plots the compensated results (±0.06°) with PZT actuation; the previous results (±0.3°) are plotted for comparison. PZT-embedded suspension is developed to assist the primary seesaw arm actuator and maintain a constant axial movement during focusing operation.

3 Design and evaluation of performance of tilt

3.1 Compensation mechanism

Figure 2a schematically depicts conventional seesaw actuation for a seesaw arm actuator; the shortcomings of optical axis tilting have been described in more detail (Hong et al. 2005; He et al. 2004). The same principle holds applies to small skew focusing. Therefore consequently, angular deviations cannot be maintained precisely perpendicular to the disc recording. Figure 2b proposes the dual-stage leverage mechanism of active tilt compensation. A tilt compensation mechanism involves a secondary micro-PZT actuator for fine focusing and a conventional VCM for coarse positioning. As display in Fig. 2, the geometric tilt angle (θ) is the angle between radial direction of seesaw arm and x-direction. The relative displacement from actuator pivot to the optical module is given by (Kim et al. 2009a, b; He et al. 2002)

$$\begin{cases} x = L_a(1+\cos\theta) + L_p \\ y = h_p + L_a \sin\theta \end{cases}. \quad (1)$$

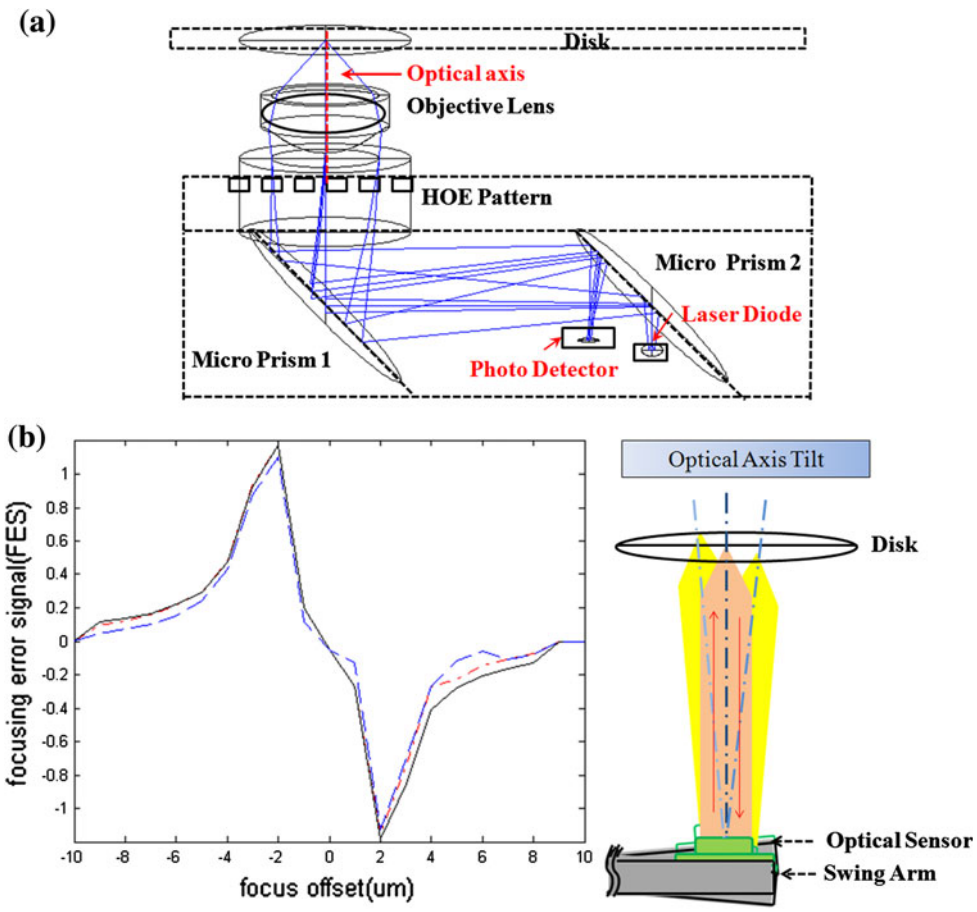

Fig. 1 **a** Integrated optical module. **b** Simulation and verification of focusing error signal: ideal (*black line*), with skew focusing mechanism (*blue line*), and with dual stage compensation (*red line*)

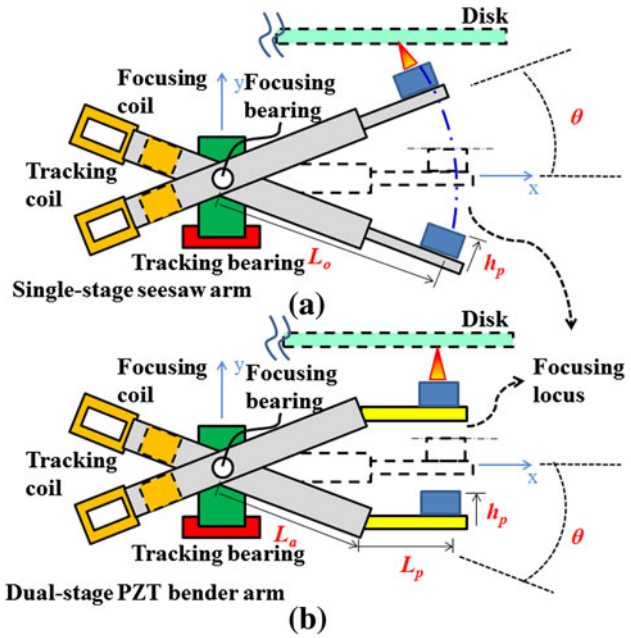

Fig. 2 Underlie actuation mechanisms. **a** Skew focusing mechanisms. **b** Dual stage actuation with PZT-embedded suspension

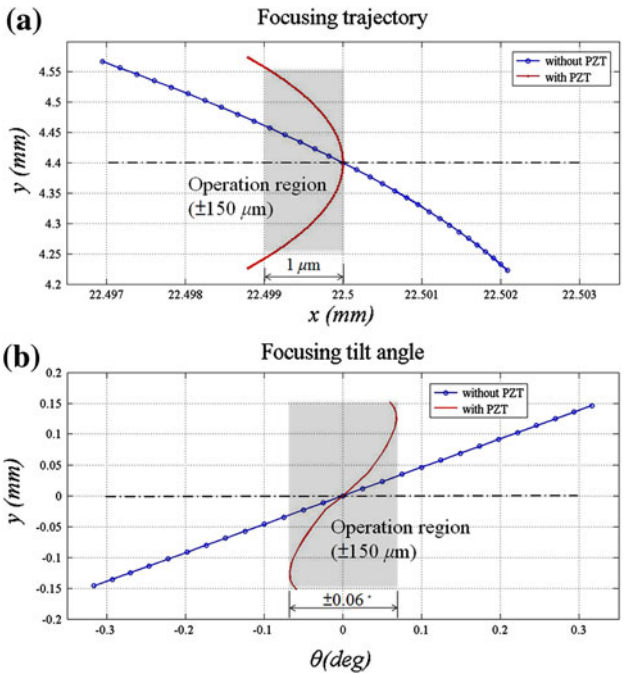

Fig. 3 Focusing operation. **a** Motion trajectories with various driving mechanisms. **b** Tilt-angle variations in focusing operation

where L_a is the distance from the actuator pivot to the front end of the seesaw arm; L_p denotes the distance from the PZT connection to the focal spot, and h_p is the height of the optical sensor above the y-axis. Hence, the trajectory motion equation for dual stage driving is

$$\left[x-(L_a+L_p)\right]^2+(y-h_p)^2=1. \tag{2}$$

Figure 3a plots the lateral displacement (x-direction) versus focusing range (y-direction) of the dual stage actuator (*red line*). The minimum lateral displacement is less than 1.5 μm when the expected focusing operating range is about 300 μm. Moreover, the trajectory motion equation for single stage driving can be evaluated from

$$x^2+y^2=L_o^2+h_p^2. \tag{3}$$

where L_o is the distance from the actuator pivot to the focal spot position. With reference to Fig. 3a (blue line), the lateral displacement exceeded 5 μm within focusing stroke. The figure indicates that the lateral displacement of a seesaw arm suspension in which is embedded a micro-PZT actuator was reduced by 80%. The angle of the optical axis offset is given by

$$\theta=\tan^{-1}\frac{(y-h_a)}{x}. \tag{4}$$

Figure 3b plots the predicted variation of the optical axis tilt with the driving mechanism, simulated in the operating region (300 μm). The operation region of dual-stage driving mechanism (*red line*) is within the minimum optical angular deviation (±0.06°) and is implemented perpendicular to the disc surface; the single-stage driving mechanism (*blue line*) is utilized at larger skew angle deviations (±0.3°) under the same conditions. To enhance the suspension dynamics, the proposed design modifies the principle of skew focusing, and thereby shortens the distance between the pickup head and the disc.

Mechanisms for enhancing read/write performance are analyzed using finite element methods (FEM) to elucidate their dynamic characteristics (modal shapes and frequency vibrations). Figure 4 reveals that the proposed design has better dynamics than the seesaw arm actuator. Mode shapes are simulated for natural frequencies of first and second modes from 0–3 kHz. The cantilever mode frequency of the present design is observed to be approximately 358 Hz, which exceeds that of the original design. The first bending mode frequency for mechanical bandwidth is improved from 281 to 2,375 Hz. According to modal analysis, the secondary micro-PZT actuator design reserves adequate bandwidth to ensure mechanical stability and enhances dynamic performance. The dual-stage actuator has a higher mechanical bandwidth when the micro-PZT bender is developed for tilt compensation.

Figure 5 shows the two prototypes of an SFF seesaw arm actuator. Figure 6 plots, and Table 1 presents, the LDV (Laser Doppler Vibormeter) measurements of the frequency response of both dual/single stage actuators. Besides, the specifications of PZT bender is shown in Table 2. Within the PZT bender, the single-stage actuator (blue line) has two resonance peaks (blue line) at 102 and 481 Hz, which are obtained from the natural mode of the

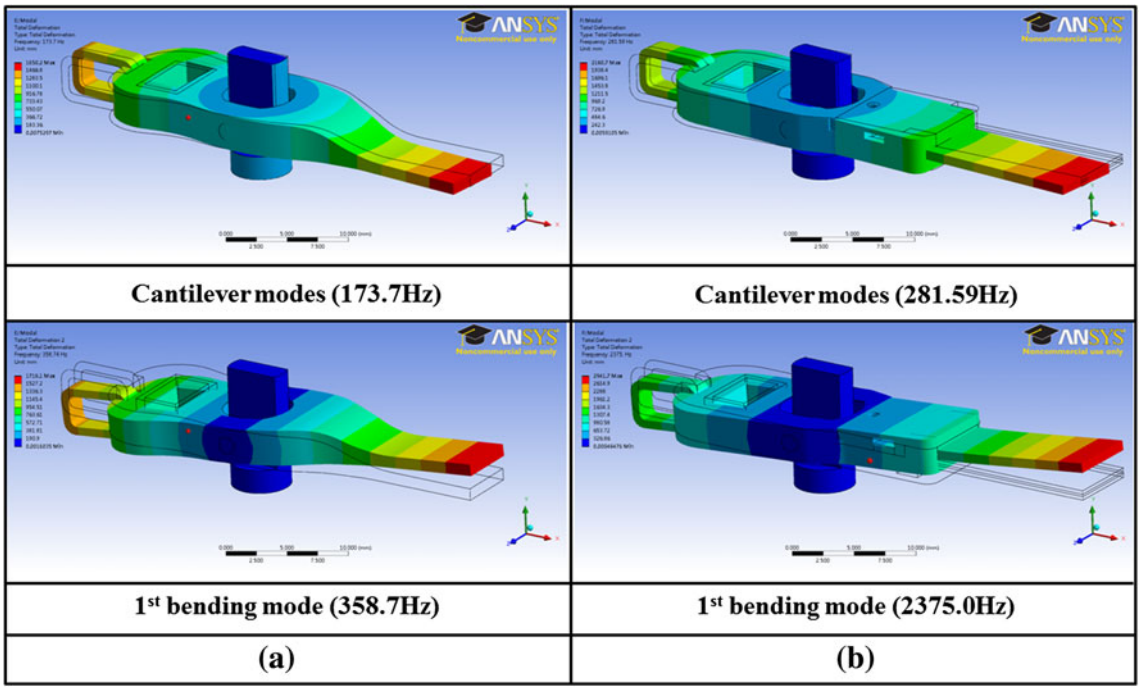

Fig. 4 Comparison of finite element models of actuator assemblies **a** single-stage seesaw actuator, **b** dual-stage PZT actuator

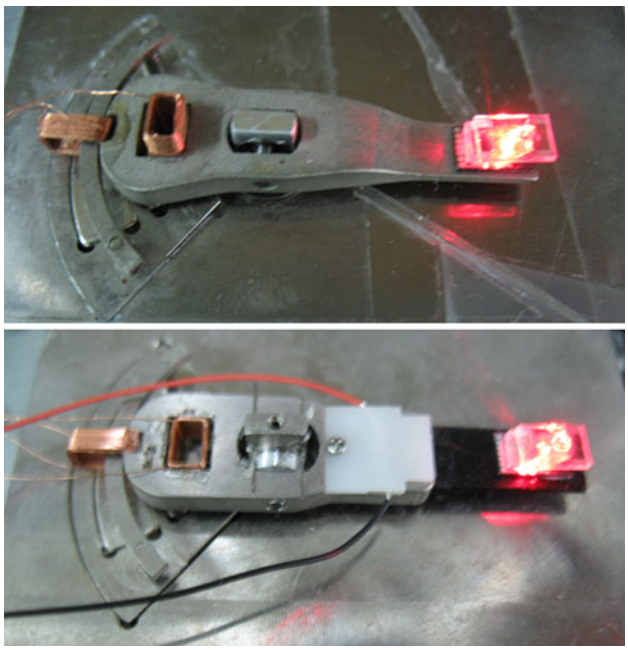

Fig. 5 Prototypes of actuator with/without PZT bender

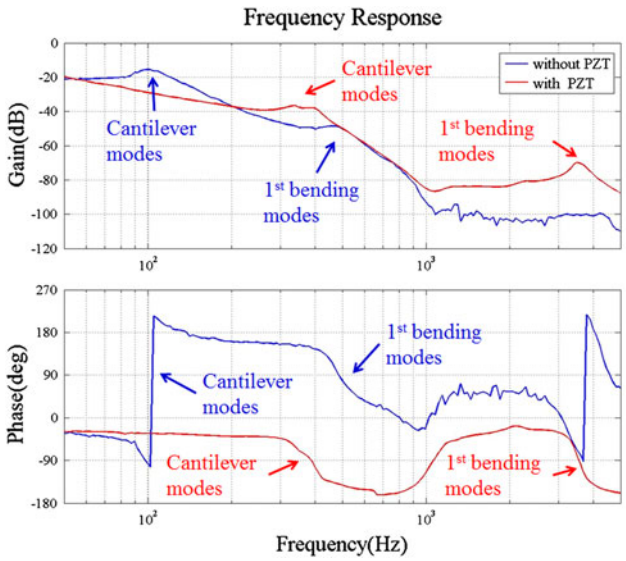

Fig. 6 Frequency response of single/dual-stage actuator

seesaw arm actuator. However, the dual-stage PZT actuator (red line) increases these two resonance frequencies at 351 and 3,459 Hz (Li et al. 2006), respectively. Accordingly, the use of PZT-embedded suspension not only increases the mechanical bandwidth but also simplifies the tilt compensation methods. Furthermore, recommendations presented its application and future developments include: (1) structural shape optimization, and (2) modeling and control strategies.

Figure 7 depicts the focusing trajectory in simulation and experiment results for comparison. In single-stage system, the real trajectory curve have maximum 10% tracking error to the ideal curve due to assembly precision. In theoritical dual-stage system, because the boundary condition of PZT is set as pinned connection, the result is a smooth curve. In fact, the real locus have 8% tracking error but within the tolerance. By this approximation, the curve

Table 1 Comparison of single/dual-stage actuators

	Single-stages seesaw actuator	Dual-stage PZT actuator
Lateral displacement	5 μm	1 μm
Focusing tilt angle	±0.3°	±0.06°
Mode shapes		
Cantilever mode	173.7 Hz	281.59 Hz
1st bending mode	358.7 Hz	2,375.0 Hz
Frequency response		
Resonance peak 1	102 Hz	351 Hz
Resonance peak 2	481 Hz	3,459 Hz

Table 2 The specifications of PZT bender

Item	Correspondence
Size (mm)	23 × 0.85 × 6
Resonance freq. (Hz)	985
Maximum input Volt (V)	150
AC sensitivity (μm/V)	300
DC sensitivity (μm/V)	450

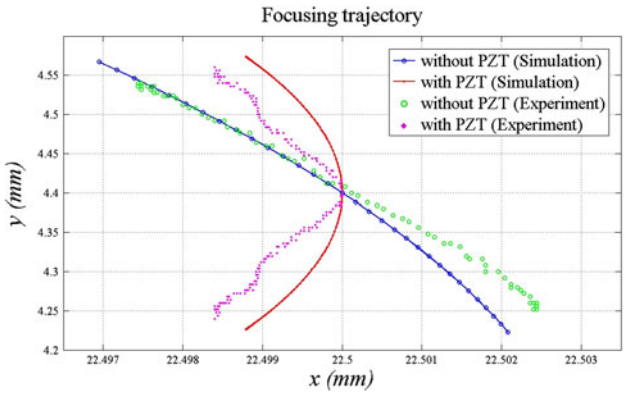

Fig. 7 Comparisons of single/dual system trajectory in experimental and simulation results

is simplify and approach the trends. Figure 8 shows the experimental FES in dual/single stage actuator which peak shift versus tilt angle. The FES of dual-stage (blue) has higher peak then single-stage (red) which closed to the idea result (Fig. 1). By applying the PZT, the linear range of FES is enlongated so the focusing range is also increased.

4 Conclusion

This work tested a dual-stage PZT seesaw arm actuator for use with an SFF pickup heas. Based on the assumption of dual-axis rotary motion, highly symmetric focusing trajectories offer stable focusing and reduce the lateral displacement approximately 80%. The tilt angle of the seesaw

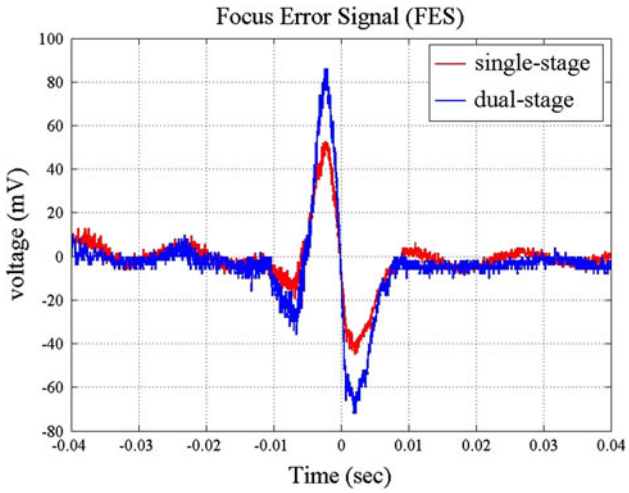

Fig. 8 Experiments and verification of focusing error signal

arm is compensated for by a mirco-PZT actuator and reduced to ±0.06°. In the simulation, the FES of the integrated optical module is improved, approaching the theoretical value. The mode shape and resonance frequency was simulated by Finite Element method (FEM). Finally, the dynamic response of the fabricated dual-stage actuator is measured using LDV. Simulation and experimental results reveal that the PZT bender substantially increases the resonance frequency. The improvements of the first and second modes increases the actuator bandwidth (from 481 to 3,459 Hz) associated with the focusing direction. In summary, this investigation demonstrates the feasibility of this SFF pickup head with a dual-stage PZT actuator device for the next generation of optical storage systems.

References

Blankenbeckler DL, Bell BW Jr, Davies DH, Lee LW (2004) Performance characteristics of a 32 mm small form-factor optical disc and drive. Jpn J Appl Phys 43:4896–4899

Cho WI, Park NC, Yang H, Park YP (2002) Swing-arm-type PZT dual actuator with fast seeking for optical disk drive. Microsyst Technol 8:139–148

Chou PC, Lin YC, Cheng C (2010a) A novel seesaw swivel actuator design and fabrication. IEEE Trans on Mag 46:2603–2610

Chou PC, Lin YC, Cheng S (2010b) Optimization of seesaw swing arm actuator design for small form factor optical disk drive. Jpn J Appl Phys 49:052502

He Z, Ong EH, Guo G (2002) Optimization of a magnetic disk drive actuator with small skew actuation. J Appl Phys 91:8709–8711

He N, Jia W, Yu D, Huang L, Gong M (2004) A novel type of 3-axis lens actuator with tilt compensation for high-density optical disc system. Sens Actuators A 115:126–132

Hong EJ, Kim DW, Park NC, Yang HS, Park YP, Kim SK (2005) Design of swing arm type actuator and suspension for micro optical disk drive. Microsyst Technol 11:1085–1093

Hou KC, Chou PC, Cheng S, Lin YJ, Chiu Yi, Chiou JC (2011) Fabrication and verification for the small-form-factor holographic optical pickup. Optical Rev 18:60–65

Kim KH, Lee Y, Kim S, Park NC, Park YP, Park KS, Yoo J, Kim CS (2009a) Numerical quasi-static analysis of ultralow flying slider during track-seeking motion over discrete track media. IEEE Trans Mag 45:4990–4993

Kim SH, Kim JH, Yang J, Yang H, Park JY, Park YP (2009b) Tilt detection and servo control method for the holographic data storage system. Microsys Technol 15:1695–1700

Knittel J, Mößner J, Bammert M (2009) A swing arm actuator for a small form factor optical drive. Microsyst Technol 15:471–476

Ko B, Jung JS, Lee SY (2006) Design of a slim-type optical pick-up actuator using PMN-PT bimorphs. Smart Mater Struct 15:1912–1918

Li Y, Marcassa F, Horowitz R, Oboe R, Evans R (2006) Track-following control with active vibration damping of a PZT-Actuated suspension dual-stage servo system. J Dyn Sys Meas Control 128:568–576

Lin YC, Chou PC, Hou KC, Cheng S, Chiou JC, Shih HF (2011) Optimizing the performance of optical data storage drives based on a novel seesaw–swivel actuator for a holographic module. Micro Nano Lett 6(7):571–574

Lee HS, Kim YH, Hwang TY, Kim CS (2005) VCM design to improve dynamic performance of an actuator in a disk drive. IEEE Trans Mag 41(2):774–778

Shih HF, Chang CL, Lee KJ, Chang CS (2005) Design of optical head with holographic optical element for small form factor drive systems. IEEE Trans Mag 41:1068–1070